International Journal of Precision Engineering and Manufacturing (2021) 22:1469–1486
https://doi.org/10.1007/s12541-021-00552-8

Online ISSN 2005-4602
Print ISSN 2234-7593

REVIEW

Rigid Precision Reducers for Machining Industrial Robots

Anh-Duc Pham[1] · Hyeong-Joon Ahn[2]

Received: 9 January 2021 / Revised: 8 June 2021 / Accepted: 8 June 2021 / Published online: 28 June 2021

Abstract

Machining robots are expected to significantly change existing production systems in the near future. The quality of the machining process with robots is mainly governed by the accuracy and stiffness of the robots. Therefore, a precision reducer for the robot joint is an important component that governs the accuracy of machining robots. This paper presents a review of rigid precision reducers for machining robots. Initially, an overview of the machining robots and their features is introduced. The importance of a precision reducer as a component of a robot for machining is explored. A cycloid reducer is the best candidate among precision reducers, considering both the structural compliance and kinematic accuracy of the machining robots. This is followed by reviews of various cycloid reducers and their operating principles. The design issues of the cycloid reducer for performance improvement are then presented. Additionally, the methodology and analysis to assess the performance of the cycloid reducers are discussed. The machining and fault detection of a cycloid reducer are briefly addressed. Finally, other applications of cycloid reducers are introduced.

Keywords Rigid precision reducer · Cycloid reducer · High stiffness reducer · Machining robot · Industrial robot

1 Introductions

Smart manufacturing is a strong industrial driver for reshaping the current competitive landscape and establishing new market leaders. Manufacturing has evolved to become more automated, computerized, and complex. Smart manufacturing can be defined as a set of technologies that employ a computer-integrated process, high levels of adaptability, rapid design changes, digital information technology, and more flexible technical workforce training [1]. Smart manufacturing allows building of new value-added processes and networks to improve and optimize the flexibility, adaptability, and efficiency of business processes.

This paper is an invited paper (Invited Review).

✉ Anh-Duc Pham
ducpham@dut.udn.vn

✉ Hyeong-Joon Ahn
ahj123@ssu.ac.kr

[1] Faculty of Mechanical Engineering, The University of Danang, University of Science and Technology, 54 Nguyen Luong Bang Street, Lien Chieu District, Danang City, Vietnam

[2] School of Mechanical Engineering, Soongsil University, 369 Sangdo-ro, Dongjak-gu, Seoul 06978, Republic of Korea

Cyber-physical systems (CPS)—a new trend in smart manufacturing-related research—integrates the cyber world and the dynamic physical world by combining computing, communication, and control [2]. The main feature is the integration of cyber-physical systems to enable intersystem communication and self-controlled system operation [3]. Moreover, smart factories integrated with CPS can be easily applied to a big data analytics platform to collect data on industrial processes [4, 5]. This would enable physical entities in smart manufacturing to be controlled and supervised in a safe, efficient, and reliable manner [6].

Additive manufacturing (AM) or three-dimensional (3D) printing is considered as a CPS owing to the interlacing of virtual production with physical production [7]. AM has introduced new production methods to design, manufacture, and distribute to end users. Moreover, AM plays an important role in smart manufacturing owing to its various benefits such as time and material savings, rapid prototyping, high efficiency, and decentralized production [8, 9].

Although AM technologies have experienced substantial growth in recent decades, machining manufacturing (MM) has played a dominant role in manufacturing. AM is highly suitable for green manufacturing owing to its advantages such as material saving and waste minimization [9]. However, it is not relevant to the manufacturing of large-scale products with metals and high-standard surface finishing [10]. In addition, AM has limitations in terms of material use, whereas MM is easy to apply because of the variety of materials available on the market. Finally, metal parts manufactured by AM require additional trimming with computer numerical control (CNC) machines in the case of a high precision finish [11].

Even though manufacturing automation has become extremely popular in the past 30 years, advances in AI and robots will ensure significant development in this field [12, 13]. AI is comparable to the brain in the automation process, with industrial machining robots being the body cells. In future factory automation, robots will play an important role in customizing the production process, including picking and placing, welding, painting, packaging and labeling, palletizing, and product inspection.

Machining robots are expected to significantly change existing production systems for a variety of reasons [14]. Many industrial robots are being utilized in the machining process to increase productivity and reduce labor costs. In general, a typical machining robot system includes a serial robotic arm with a machining tool attached to the end-effector of the robot [15]. Compared to traditional machining systems, these machining robots can easily expand the workspace having additional mobile platforms attached [16]. The rise of machining robots in modern factories is undeniable. In particular, 78% of industrial robot productivity in the market is used in welding and handling operations, of which more than 40% is used in the automotive and metal processing industries [17]. However, these machining robots have diverse applications because the tools mounted on the end-effector easily can be changed for different tasks, such as grinding and welding [18].

The quality of the machining process with robots is mainly governed by the accuracy and stiffness of the robots [19]. There are three types of errors affecting the accuracy of a robot: errors due to the working environment, machining process errors, and robot self-dependent errors [20]. The errors in a robot due to structural deformations of load-transmitting components, links, energy-transforming devices, or wear and nonlinear effects are hardly controllable [13, 20]. However, some of the self-dependent errors in a robot can be compensated for by suitable control or dedicated calibration [21].

The precision reducer is an important component governing the accuracy of the machining robot. High-quality mechanical and electrical parts can be used to improve the accuracy of the robot to obtain the best precision. Among these, precision reducers used in joint actuators contribute significantly to the kinematic and nongeometrical position errors of robots [22].

This paper presents a review of rigid precision reducers of industrial robots for machining. Initially, an overview of the machining robots and their features are introduced. The importance of a precision reducer as a key component of a robot for machining is explored. A cycloid reducer is the best candidate among precision reducers, considering both the structural compliance and kinematic accuracy of the machining robots. Various cycloid reducers and their operating principles are reviewed. The design issues of the cycloid reducer for performance improvement are presented. Additionally, the methodology and analysis for assessing the performance of the cycloid reducers are discussed. Afterward, the machining and fault detection of a cycloid reducer are briefly presented. Finally, other applications of cycloid reducers are introduced.

2 Machining Robot and its Characteristics

Prototypical machining robots—6-or 7-degree-of-freedom (DOF) structures of industrial robotic arms—have been used for various tasks such as milling, grilling, polishing, and cutting. An example of a 6-DOF robotic arm for the milling process is shown in Fig. 1 [23]. In this task, a machining tool is attached to the end-effector of an industrial robot. The tool can be conveniently changed on the spindle attached to the end-effector of the robot to execute other machining tasks [16]. Various studies on machining robots are presented in Table 1 [24].

The machining robot system offers many advantages over conventional CNC machines, as shown in Table 2 [25, 26]. Primarily, the workspace of the machining robot is very large and can be shared owing to the high flexibility of their arms [27]. As a result, complex bulky 3D shapes, such as an aircraft, can be machined directly with the robot. Moreover, a tool path for its smoothness can be further optimized using

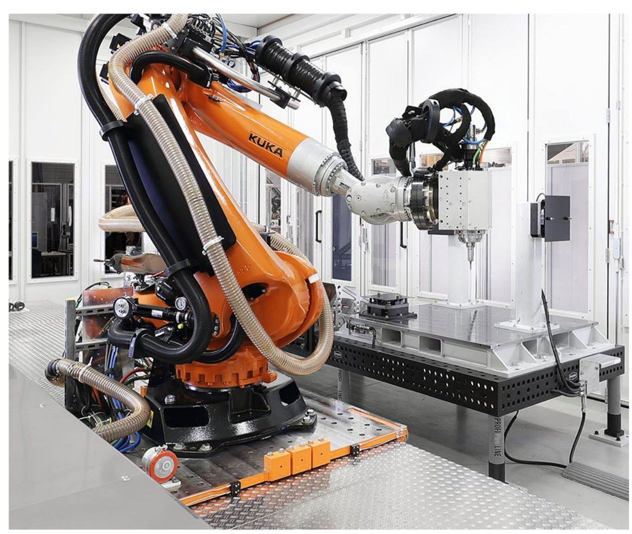

Fig. 1 KUKA milling robot [23] (open accessed)

Table 1 Applications of machining robot in different manufacturing fields [24]

Fields	Process	Product
Foundries	Deburring, milling, routing, drilling, finishing	Mold and dies, casting
Automotive	Milling, de-flashing, drilling, grinding, cutting	Engines, vehicle frame, body panels, bumpers, door-knobs, stamping dies, sand cores
Aerospace	Grinding, drilling polishing, cutting	Turbine blades, wing segments, bulkheads, insulation
Medical equipment	Grinding, polishing	Prosthesis

Table 2 Comparison between machining robots and CNC machines

Properties	Machining robots	CNC machines
Overall		
Kinematic architecture	Serial	Cartesian
Number of axes	6+	3 or 5
Kinematic redundancy	At least 1-DOF	None
Dynamic properties	Heterogeneous within the workspace	Homogeneous within the workspace
Control algorithm	Point-to-point control Continues path control	Continues path control
Error compensation	Mechanical: gravity compensators Control algorithms: Off-line and/or on-line	Not required
Actuator feedback	Single or double encoder	Single encoder
	Advantage	*Disadvantage*
Workspace	Large	Limited
Extendable capacity	Possible with extra actuators or mobile platform	Impossible
Flexibility	High	Low
Working objects	Highly flexible (easily machining oversize elements)	Limited (just for the limited size of elements)
Complexity of trajectory	Any complex trajectory	Just suitable for 3/5 axes machining
Machine operator workload	Any type of operation Several parts at one	Single or several similar operations One part at the time
Maintenance	Simple	Complex
User-friendly	Without programming knowledge	Need programming knowledge
Price	Competitive for 6-DOF robot	Competitive for 3-axes machine Expensive for a 5-axes machine
Accuracy	± 0.1 to ± 1 mm	± 0.005 mm
Repeatability	± 0.03 to ± 0.3 mm	± 0.002 mm
Mechanical compliance	Relatively low	Relatively high
The relation between actuated and operation space	Non-linear	Linear

redundant joint actuators, although trajectory planning is significantly complex compared to conventional CNC. Time and substantial effort are required to train operators who have little or no software knowledge can be saved by using the robot system.

Operational accuracy and structural stiffness are crucial in machining robots. During processes with negligible machining forces, such as welding or routing, only kinematic position errors need to be considered [28]. Compliance is very important in resisting the structural deformation caused by machining forces during the cutting or milling process [29]. Some methods have been proposed to improve the operational accuracy and structural stiffness of machining robots [21, 29]. The spindle of the robot is directly attached to its fifth joint to reduce the effect of the machining forces, which limits the flexibility and workspace of the robot [16]. Compliance compensation also helps to improve the performance of a machining robot with kinematic position and nongeometrical errors. Nevertheless, the control system of machining robots is extremely expensive and complicated because several high-resolution sensors and tracker-checking systems are required [30].

Choice of proper components in the machining robot is crucial for reducing compliance issues. The ability and performance of robots are influenced by the working environment, accuracy of the robot control system, and robot dependent errors (both kinetics and dynamics) [20]. While factors such as the working environment and control system accuracy can be adjusted during robot operation [21, 22, 28], the robot-dependence errors need to be considered in the robot manufacturing process. Robot-dependence errors include geometrical and nongeometrical errors [20]. Most of the geometrical errors result from the quality of actuators located in the joints of the robot, which is a combination of motors and high-precision reducers [31, 32]. Furthermore, nongeometrical errors are caused by stick–slip motion, hysteresis, and nonlinear deformation due to impact and cutting forces during robot operations [20, 33]. The robot joints need to be integrated with a reducer with a high torsional stiffness and the ability for long-term operation in environments requiring high-speed performance [34, 35] to minimize nongeometrical impacts. Therefore, it is extremely important to choose a reducer with good structure, high torsional rigidity, high-speed operatability with a large payload ratio, and antivibration ability during machining [14]. Examples of reducers in the machining robot are compared in Table 3 [34, 35].

3 Overview of Rigid Precision Reducers Used in the Actuator of the Machining Robot

Although several types of precision reducers are used in industrial robots [36], reducers with cycloidal disk and eccentric shaft are ideal for machining robots. Compared with a planetary reducer [37], the cycloid reducer can easily achieve a high reduction ratio without occupying a large working space. Owing to its circular tooth profile and multiple contact points, the cycloid reducer can work more efficiently and accurately than the planetary reducer. As shown in Table 3, the cycloid reducer has a much higher torque-to-weight ratio than the planetary reducer in a similar reduction ratio range, while still working with maximum efficiency under high-speed conditions. There is the other possible option for a joint reducer with a harmonic drive [35]. However, the harmonic drive has a continuously deformed and moving thin-wall structure causing it to have low torsional rigidity. This makes it suitable for applications with low load capacity and narrow space. [38]. The cycloid reducer is desirable for the machining robot under conditions requiring high accuracy and payload capacity, such as machining. Furthermore, the cycloid reducer is also known to exhibit high robustness and torsional stiffness with low required maintenance [34].

Table 3 Effects of the reducer on the performance of the machining robot [34, 35]

Effects on performance of machining robot	Performance index	Cycloid reducer			Harmonic drive	Planetary reducer
		Nabtesco RV-25N	Spinea-Twinspin TS110	Sumitomo Fine Cyclo F2C-T155	CSG-25-160-2UJ-LW	Wittenstein-Alpha SP^{+}075MF (2 stage)
Payload capacity, speed	Transmission ratio	1:108	1:119	1:118	1:100	1:100
	Acceleraton/nominal torques	612/245 Nm	244/122 Nm	417/167 Nm	204/87 Nm	105/84 Nm
	Torque-to-weight ratios	161/64 Nm/kg	64/32 Nm/kg	87/29 Nm/kg	208/79 Nm/kg	35/28 Nm/kg
	Efficiency and subjective dependency on operatiing conditions	87%, high (speed and torque)	74%, high (speed and torque)	87%, high (speed and torque)	84%, high (speed and torque)	94%, low (speed and torque)
Accuracy; repeatability; fast accelaracy; smooth trajectory	Backlash	< 1 Arcmin	< 1 Arcmin	< 0.75 Arcmin	0	4–6 Arcmin
	Lost motion	< 1 Arcmin	< 1 Arcmin	< 0.75 Arcmin	< 1 Arcmin	4–6 Arcmin
	Maximum input speed	–	4500 rpm	8500 rpm	7500 rpm	8500 rpm
	Torsional rigidity	61 Nm/Arcmin	> 22 Nm/Arcmin	25–41 Nm/Arcmin	11–16 Nm/Arcmin	10 Nm/Arcm

3.1 Operating Principle

Depending on the specific requirements of the applications, the cycloid reducer may have various structures, as shown in Fig. 2. The kinematic diagram of the cycloid reducer can be divided into five types: 2K-H, K-H-V, rotate vector (RV), China Bearing Reducer (CBR), and output-pin-wheel. The 2K-H type cycloid reducer consists of a planet carrier (H) and two central gears (K), as illustrated in Fig. 2a [39]. However, the 2K-H type cycloid reducer may have a high reduction ratio but low efficiency because it always need at least two gear pairs to transfer movement between input and output [40]. Thus, the K-H-V type cycloid reducer was invented to overcome the drawback of the 2K-H type by introducing an equal angular mechanism (V). The K-H-V type cycloid reducer is compact, lightweight, and highly efficient (Fig. 2b) [41]. The RV-type cycloid reducer using a combination of K-H and K-H-V cycloid reducers is proposed, as shown in Fig. 2c, to further increase the reduction ratio and enhance the flexibility of the output input [36]. Recently, a CBR-type cycloid reducer (Fig. 2d) was suggested for minimizing the volume; the outer diameter of the cycloid reducer would be similar in size to the harmonic drive [42]. The CBR-type cycloid reducer has disc connectors instead of the pin roller in the K-H-V-type cycloid reducer. Furthermore, an output-pin-wheel mechanism that works by switching functions between the output and housing using four cycloid disks, as shown in Fig. 2e, is proposed [43]. The kinematic diagram of the output-pin-wheel reducer is similar to that of the K-H type. Furthermore, the installed size can be increased. In general, the RV type cycloid reducer is the most widely used option in industrial robots nowadays.

3.2 Design Optimizations of the Cycloid Reducer

Design optimization is key to improving the performance of cycloid reducers. The performance of the cycloid reducer can be improved by using materials, lubrication

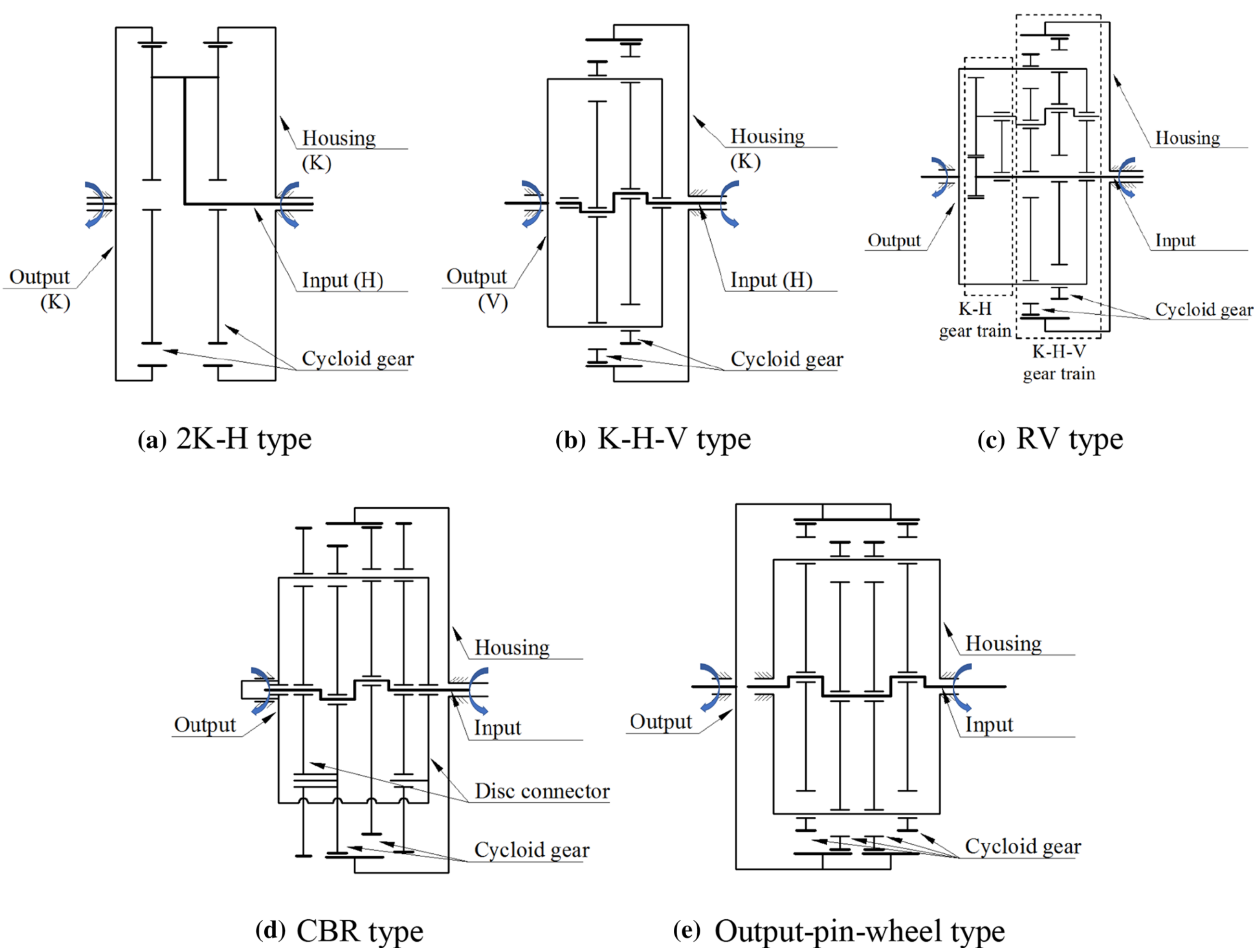

Fig. 2 Operating principle of various cycloid reducers

methods, and design optimization. Various materials, from low-carbon steels to high-quality alloy steel, are used for cycloid reducers [44]. Alloy steels with Mn and Cr are widely used because of their hardenability, high bending strength, and fatigue strength [45]. Although Al is used in some parts of the harmonic drive owing to its lightweight, material choices for the cycloid reducer are limited because they have to guarantee structural stiffness of the reducer. Oil, grease, and mixed lubrication methods for cycloid reducers have advanced over the years [46, 47]. However, research related to the optimization of cycloid designs, since the first appearance of the cycloid reducer (over 60 years ago) (structure, tooth profile, etc.), is still ongoing from [48].

Design optimizations for cycloid reducers can be classified into three main groups: generating method of tooth profile, modification or correlation of the profile, and structural design. Several methods have been proposed to generate a cycloid profile for manufacturability. Tooth profile modifications or corrections are proposed to minimize the gaps between engaging elements. In particular, minimizing the initial gap (ideally 0) between engaged teeth pairs can significantly decrease transmission errors between output and input, which increases the accuracy of reducer. Lastly, most research related to reducer designs concentrates on the structural optimization of the cycloid reducer.

Methods for generating the cycloid tooth profile are divided into three main categories: circle enveloping [41, 49], transmitted coordinate systems [50–52], and instant-velocity center method [53, 54], as shown in Fig. 3. The circle-enveloping method generates a trace of a point of a circle rolling on the other fixed circle, which is called an epitrochoid curve, in coordinate system F_x (O_x, X, Y) [41]. The transmitted coordinate system method generates the

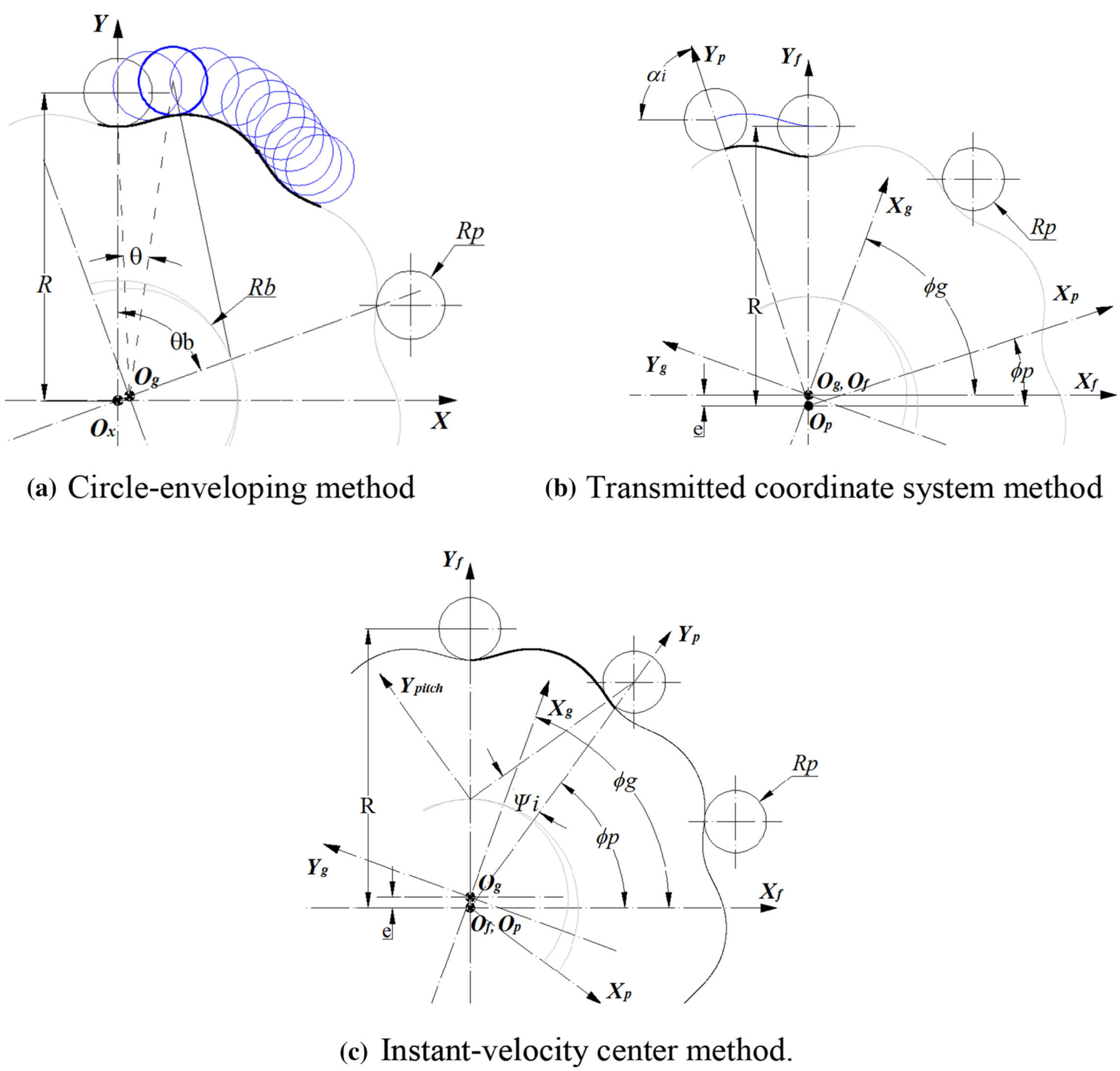

Fig. 3 Generating methods of cycloid tooth profile

Table 4 Equations for cycloid tooth profile with different methods

Circle-enveloping method [41]	Transmitted coordinate system method [56]	Instant velocity center method [53]
Point on epicycloid curve: $\begin{cases} x_c = R\left(\sin\theta - \frac{R_b}{RZ_p}\sin Z_p\theta\right) \\ y_c = R\left(\cos\theta - \frac{R_b}{RZ_p}\cos Z_p\theta\right) \end{cases}$ Curvature radius of epicycloid curve: $\rho_c = \frac{R/K\left(1+K^2-2K\cos\theta_b\right)^{2/3}}{(1+Z_p)\cos\theta_b-(1+Z_pK^2)}$ $(K=R_b/R)$ with: *R:* Radius of the pin-roller distributed circle R_b: Pitch radius of the pin-roller distributed circle Z_p: Number of pin-roller of the cycloid reducer θ: Rotation angle of pin-roller around center O_g θ_b: Rotation angle of pin-roller around center O_x R_p: radius of the pin-roller	Point on epicycloid curve: $\begin{cases} x_c(\alpha_i,\phi_p) = R\sin(\theta_i - \phi_p + \phi_g) \\ \quad +R_p\sin(\alpha_i + \phi_p - \phi_g - \theta_i) \\ \quad -e\sin\phi_g \\ y_c(\alpha_i,\phi_p) = R\cos(\theta_i - \phi_p + \phi_g) \\ \quad -R_p\cos(\alpha_i + \phi_p - \phi_g - \theta_i) \\ \quad -e\cos\phi_g \end{cases}$ Curvature radius of epicycloid curve: $\rho_c(\alpha_i,\phi_p) = \begin{bmatrix} x_c(\alpha_i,\phi_p) \\ y_c(\alpha_i,\phi_p) \\ 1 \end{bmatrix}$ with: ϕ_p, ϕ_g: angular movement of coordinate systems F_p and F_g in comparison with F_x α_i: the angle between the vertical axis of F_p and horizontal axis of F_x θ_i: the position of ith pin-roller in coordinate system F_x *R:* Radius of the pin-roller distributed circle R_p: radius of the pin-roller *e*: eccentricity	Point on epicycloid curve: $\begin{cases} x_c = R\cos(\phi_g - \phi_p) \\ \quad -R_p\cos(\phi_g - \phi_p - \psi_i) \\ \quad -e\cos\phi_g \\ y_c = -R\sin(\phi_g - \phi_p) \\ \quad +R_p\sin(\phi_g - \phi_p - \psi_i) \\ \quad +e\sin\phi_g \end{cases}$ Curvature radius of epicycloid curve: $\rho_c = \begin{bmatrix} x_c \\ y_c \\ 1 \end{bmatrix}$ with: ϕ_p, ϕ_g: angular movement of coordinate systems F_p and F_g in comparison with F_x ψ_i: Pressure angle between ith pin-roller and the cycloid gear *R:* Radius of the pin-roller distributed circle R_p: radius of the pin-roller *e*: eccentricity

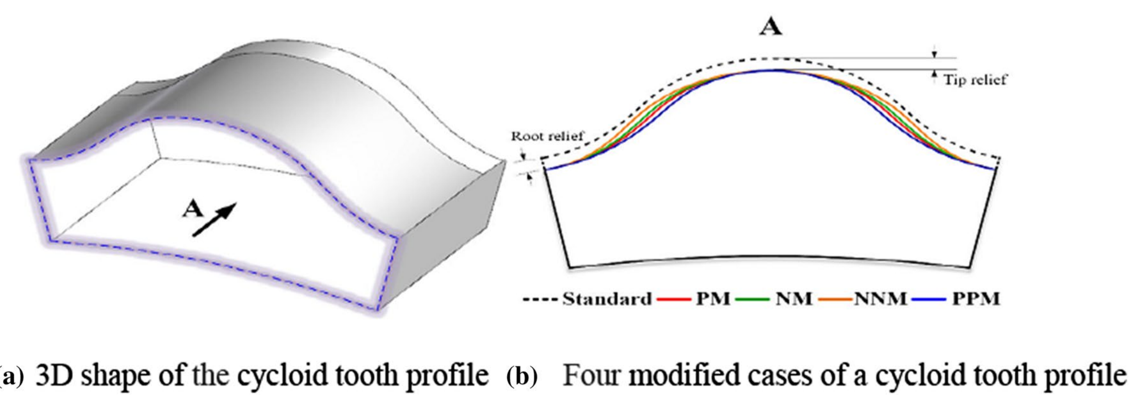

Fig. 4 Cases of profile modifications of the cycloid reducer [64] (open accessed). **a** 3D shape of the cycloid tooth profile, **b** Four modified cases of a cycloid tooth profile. *PM: positive roller radius modification; NM: negative roller position modification. NNM: negative roller position and negative roller radius modification. PPM: positive roller position and positive roller radius modification

epitrochoid curve by transforming points in the coordinate system with different frames of reference. This method normally uses three frames of reference F_g (O_g, X_g, Y_g), F_p (O_p, X_p, Y_p), F_f (O_f, X_f, Y_f) that are attached to the cycloid disk, cycloid pin (or cycloid wheel), and fixed-frame or housing [55–57]. The F_p of a cycloid pin coincides with F_f, whereas F_p revolves around the origin of F_f, as illustrated in Fig. 3b. The instant-velocity center method utilizes three frames of reference similar to the transmitted coordinate system method and one more frame for the pitch point of the cycloid reducer (instant-velocity center). Thus, the generated epicycloid curve is determined according to the positions of the pitch point and contact point of the conjugating surfaces between the cycloid reducer and cycloid pins [53]. A comparison among the generating equations used in the three methods is presented in Table 4. The shape of the designed cycloid disk or the epicycloid curve depends on the radius of the pin roller, radius of the circle passing through the centers of the pin-rollers, eccentricity, number of pin-rollers, and number of teeth (or lobes of the profile) of the cycloid reducer.

Modifications or corrections of the tooth profile should be performed to tolerate errors during both assembly and manufacturing processes [58, 59]. A small change in the theoretical tooth profile is made at the conjugated section of the tooth contact. Modifications or corrections of the tooth profile guarantee smooth engagement, increase the contact number, and provide good lubrication conditions [60, 61]. There are two types of tooth modification methods: single modified parameter and multi-modified parameter methods. The isometric, offset, and angular rotation modifications correspond to the single modified parameter method [54, 62]. Isometric and offset modifications are used to adjust the radius of the pin roller and the radius of the circle passing through the center of the pin rollers, respectively [62–64]. In contrast, the angular rotation modification changes the center position of the pin rollers along the circumferential direction [54, 62]. Isometric and offset modifications can be applied independently [63] or together [58], whereas the angular rotation modification can only be applied along with other methods [54]. Examples of single modified parameter and multimodified parameter methods are shown in Fig. 4 [64]. A comparison between various cases of a modified cycloid tooth profile with a theoretical profile is introduced by sole isometric modification (both positive and negative), and a combination of isometric and offset modifications. Furthermore, the multimodified parameter method of changing the tooth shape considering the pressure angle [59], increasing contact points [55], or under-cutting phenomenon [57] are presented. Finally, a tooth modification method is studied as a unified process of combining parameters such as machining tolerances and axial play in bearings [65].

Various design problems of the cycloid reducer have been studied because the structure of a cycloid reducer has a significant effect on its performance [39, 52, 59]. As mentioned in the previous section, five types of cycloid reducers are introduced to improve their performance, including size, payload, strength, and stiffness [52, 66]. Furthermore, the output mechanism of a cycloid reducer has a significant impact on the torsional stiffness and vibration [67–69]. A cycloid reducer structure without pin rollers was proposed to decrease the stress fluctuation associated with conventional designs [70]. This research also recognized that the presence of more than two tooth differences reduces stress fluctuations and velocity ripple, in addition to improving the stress distributions of the cycloid reducer. In contrast, reducing the difference in tooth number between two pin-rollers of the 2K-H type cycloid reducer can improve the self-locking performance of the mechanism but degrade the backlash angle of the reducer [39].

All aspects of the tooth profile and the cycloid reducer designs are summarized in Fig. 5.

4 Performance Analysis of the Cycloid Reducer

Internal and external factors affecting the performance of the cycloid reducer, as shown in Fig. 6. The tooth geometry and bearing characteristics are the most significant internal factors affecting the load capacity, rigidity, bending stress, and torque ripple of the transmission device [71]. On the other hand, machining errors or tolerances of the components of a cycloid reducer increase backlash, lost motion, and transmission errors, in addition to causing vibration and noise in the system [58, 72]. Nevertheless, both the payload and speed are external factors that significantly influence the efficiency of the reducer, whereas the assembling misalignment between the reducer and input or output parts affect the vibration/noise and shock resistance of the system [73, 74].

A mathematical model of the contact point and force distribution of a cycloid reducer is required, considering that the contact force distribution is a fundamental in investigating tooth stress and dynamic transmission performance analysis. Dynamic equations for the contact force distribution in the meshing area of a 2K-H cycloid reducer are derived in [39]. A detailed analysis of the dynamic model of the eccentric shaft bearing is performed to evaluate the engagement of a cycloid reducer [75, 76]. Recently, stress analysis of a cycloid reducer was performed by combining the kinematics and dynamics of rigid bodies and nonlinear stiffness based on contact dynamics [77].

As mentioned in the previous section, the structures of the reducer as well as the tooth profile and its modification strongly affect the force distribution, hysteresis curve, transmission errors, and efficiency [67]. The contact number and force distribution of a cycloid reducer are numerically studied considering two tooth modification methods, i.e., isometric and offset methods, and their effects on the torque performance of the cycloid reducer are analyzed [64]. Tooth profile modifications based on the contact angle (straight line, catenary, and cycloid functions) reduce the backlash and lost motion of the cycloid reducer significantly compared to conventional tooth modifications, as shown in Fig. 7 [59]. In addition, high stress concentrated on the contact points of a cycloid reducer such as pin-rollers could be relieved by performing FE analysis and design modifications [78, 79]. Longitudinal tooth profile modifications are also effective in smoothing the contact distribution [64, 80] as well as performance—efficiency [66], transmission error [60, 76], and torsional

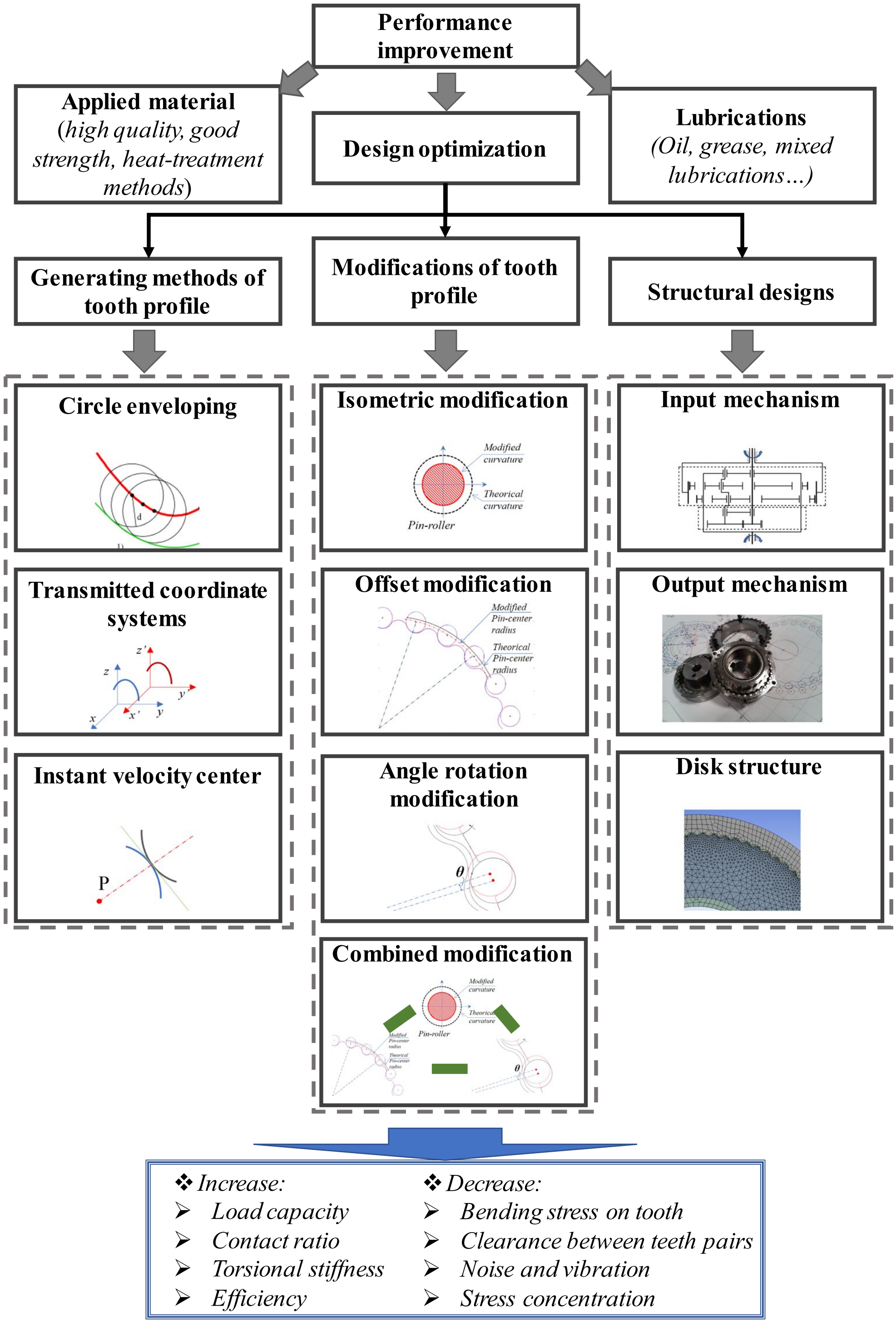

Fig. 5 Design optimizations of the cycloid reducer

rigidity [81]. As an example, the transmission error of an RV-type reducer can be reduced by 24%, with proper tooth modification, as shown in Fig. 8 [52]. The nonpin A cycloid reducer without pinwheels [51] might exhibit higher efficiency under certain conditions than those with pinwheels [82].

Bearings used in a cycloid reducer significantly influence the performance of the cycloid reducer, which can be studied using numerical or FEM analysis [83]. In particular, the

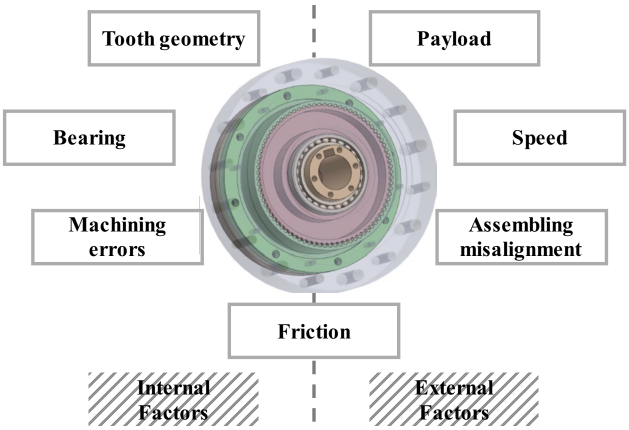

Fig. 6 Factors affecting the performance of a cycloid reducer

RV-type reducer has many bearings, making it suitable for investigating the effects of bearings on the dynamic performance of reducer [76, 84, 85]. The stiffness and geometric deflects of bearings may affect the contact force distribution and finally lead to an improvement in the vibration sensitivity and reliability of the cycloid reducer [75, 85]. Moreover, the clearance of the support bearings might affect the transmission errors of a cycloid reducer [84]. Lastly, a cycloid reducer with needle roller bearings has better efficiency than that with sleeve bearings [86].

The machining quality of the tooth profile is also a significant contributor to the performance of cycloid reducers [87, 88]. Specifically, the torsional stiffness of a cycloid gear is strongly related to the roughness of the tooth surface [87]. In addition, the clearances of the cycloid reducer due to machining errors have an impact on the hysteresis curve of the reducer, such as backlash and lost motion [88]. Finally, the manufacturing tolerance of eccentricity might also affect the force distribution and power losses of a cycloid reducer [74].

The efficiency and life cycle of the cycloid reducer are governed by friction and lubricants. The friction forces of both sliding and rolling motions cause losses in the cycloid reducer [69]. Experiments were conducted to investigate the correlation between the friction/lubricant and power losses/efficiency of the cycloid reducer [86]. As the speed increases, the friction coefficient [89] and the contact ratio decrease [61]. The contact force distribution of a cycloid reducer also influences the average film thickness and efficiency of the reducer [61]. Oil lubrication enables a large compound cycloid reducer to dissipate heat effectively from friction loss [90]. Furthermore, oil filling can be used in diagnosing a cycloid reducer, and abrasive friction particles should be carefully checked to extend the life cycle of the cycloid reducer [91].

The performances of the cycloid reducers are investigated experimentally, as shown in Figs. 9 and 10. The experimental setup is divided into four principal subsystems: assembly, instrumentation, supervision, and interface, as shown in Fig. 9. All components connected in the transmission system are denoted by "assembly." “Instrumentation” includes high precision sensors, such as an angle encoder, torque meter, and speed meter. Usually, the control system drives the input angle of the motor through a motor driver and applies a torque load via a brake or servomotor. Finally, the "interface" helps to collect and show the data. All data from "instrumentation" are collected and displayed on a computer.

The impacts of operating payload, speed, and misalignment errors on the performance of the cycloid reducer can be experimentally studied. Integrated with internal effects, an experimental system with a precision reducer might operate with slightly lower performance, including having higher transmission error [71, 73], lower torsional stiffness [67, 92], and more vibrations [92, 93]. Even though the efficiency could be improved under certain conditions, such as high input torque and low speed, many losses would still be

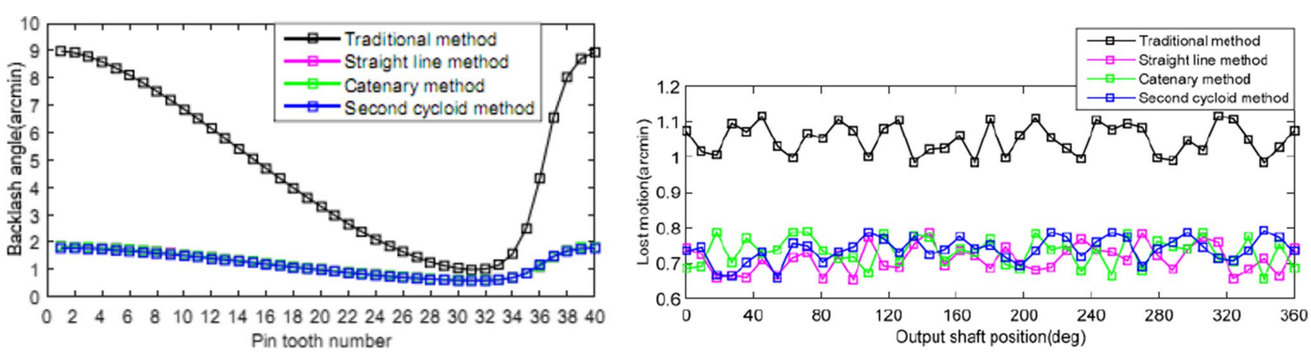

(a) Backlash **(b)** Lost motion

Fig. 7 Influence of modified tooth profile methods on the backlash and lost motion of a cycloid reducer [59] (open access)

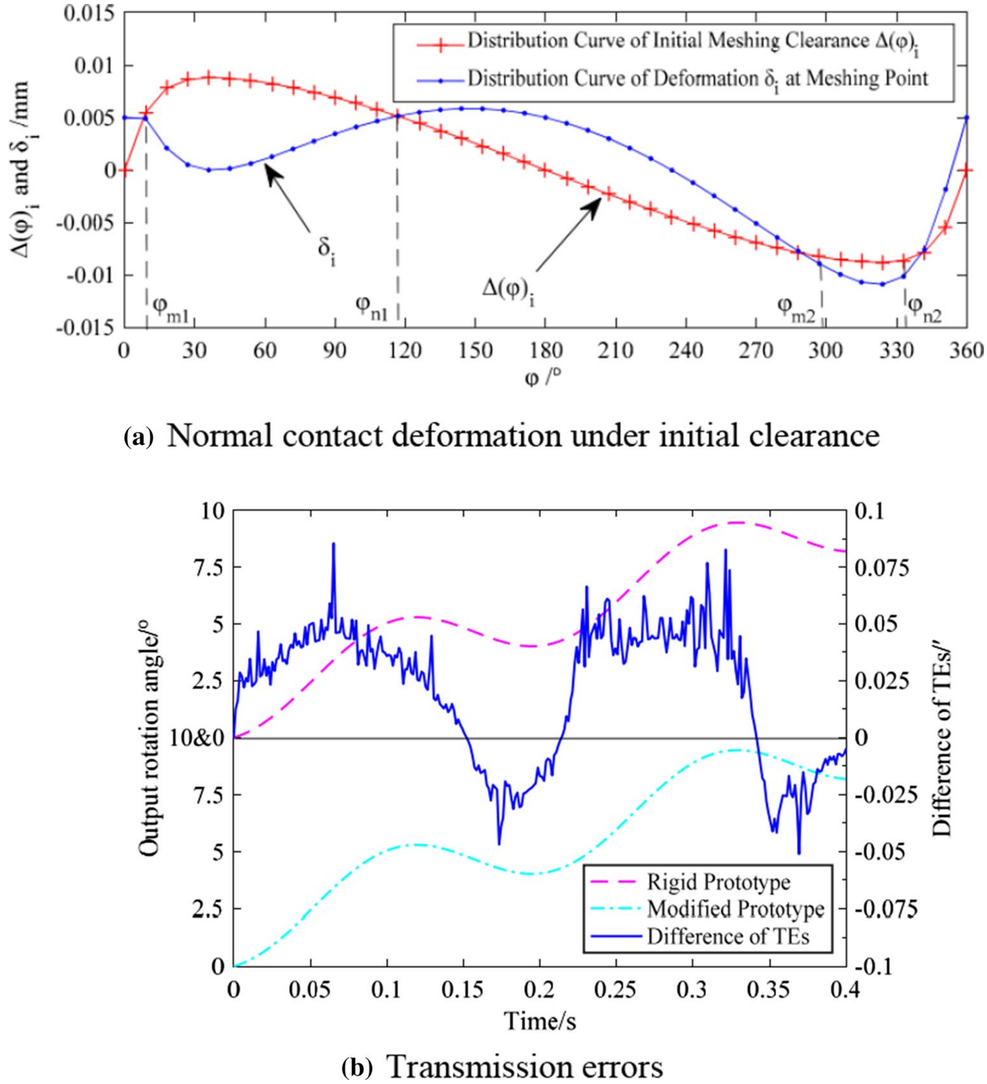

Fig. 8 Initial clearances, normal contact deformations, and transmission errors of a proposed tooth profile [52] (open access)

present in the entire experimental system [86, 89]. Thus, vibration suppression and suitable lubrication approaches would have to be carefully considered to improve the experimental conditions of the cycloid reducer [73, 91].

5 Machining Process and Fault Detections of the Cycloid Reducer

Grinding is the principal method for producing an accurate epicycloid profile of a cycloid reducer [94]. Generally, the milling process with a 5-axis CNC machine can create the tooth profile of a cycloid gear [95], but the grinding process can provide better roughness for the tooth surface of a cycloid gear [87]. With the recent improvement in precision measurement technology and gear grinding devices [96], all technical aspects of forming a complex surface, such as an epicycloid, can be handled using the grinding process. A grinding system for cycloid gear quantitatively corrects the error of the tooth profile of a cycloid reducer, with an eccentric shaft and pin rollers. The only difference is that one of the pin rollers is replaced with the grinding wheel, as shown in Fig. 11 [94].

In addition, selective parts of cycloid reducers are assembled using a genetic algorithm for better performance [97]. A fault detection method is applied to discard poor quality products of cycloid reducers [98], which are usually based on vibration signals [99] or acoustic emission [100, 101].

Fig. 9 Principal subsystems of an experimental setup of a cycloid reducer

6 Other Applications of Rigid Precision Reducer

Owing to their high-performance characteristics such as accuracy, reliability, and rigidity, cycloid reducers are widely being used in various applications, as illustrated in Fig. 12. First, a cycloid reducer is designed with an extremely compact size and unified with a servomotor in a light-weight actuator, which is suitable for mobile robots [102–104]. Moreover, medical equipment and surgical robots use a cycloid reducer as a component in an automatic tool changer or actuator [105]. In the automotive industry, a cycloid reducer is used in E-CVVT [106, 107] or the new upgraded system E-CVVD [108] as an actuator. In addition, a cycloid reducer is used as an actuator in vehilce radar systems [109].

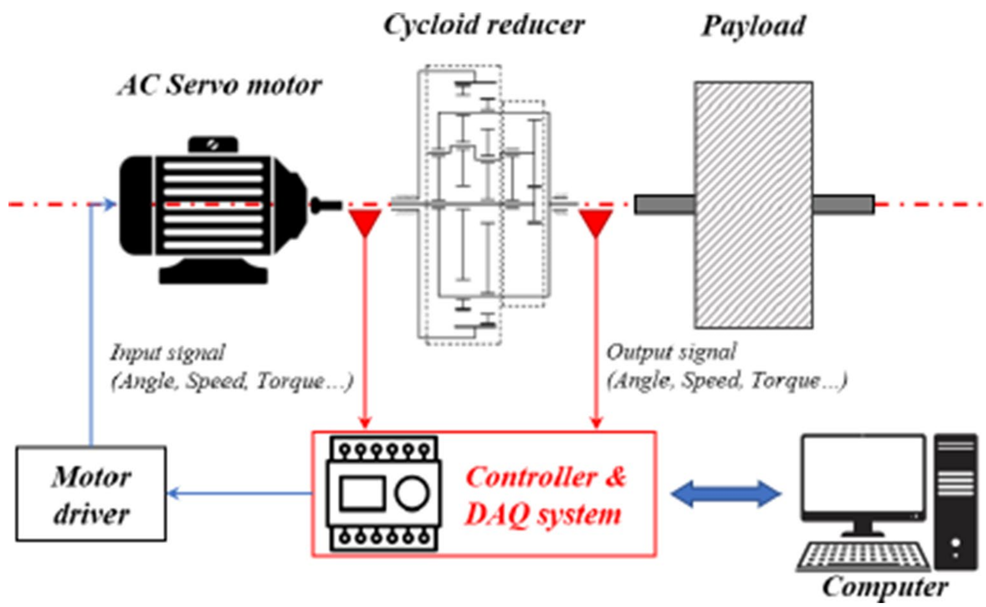

Fig. 10 Schematic of an experimental system of a cycloid reducer

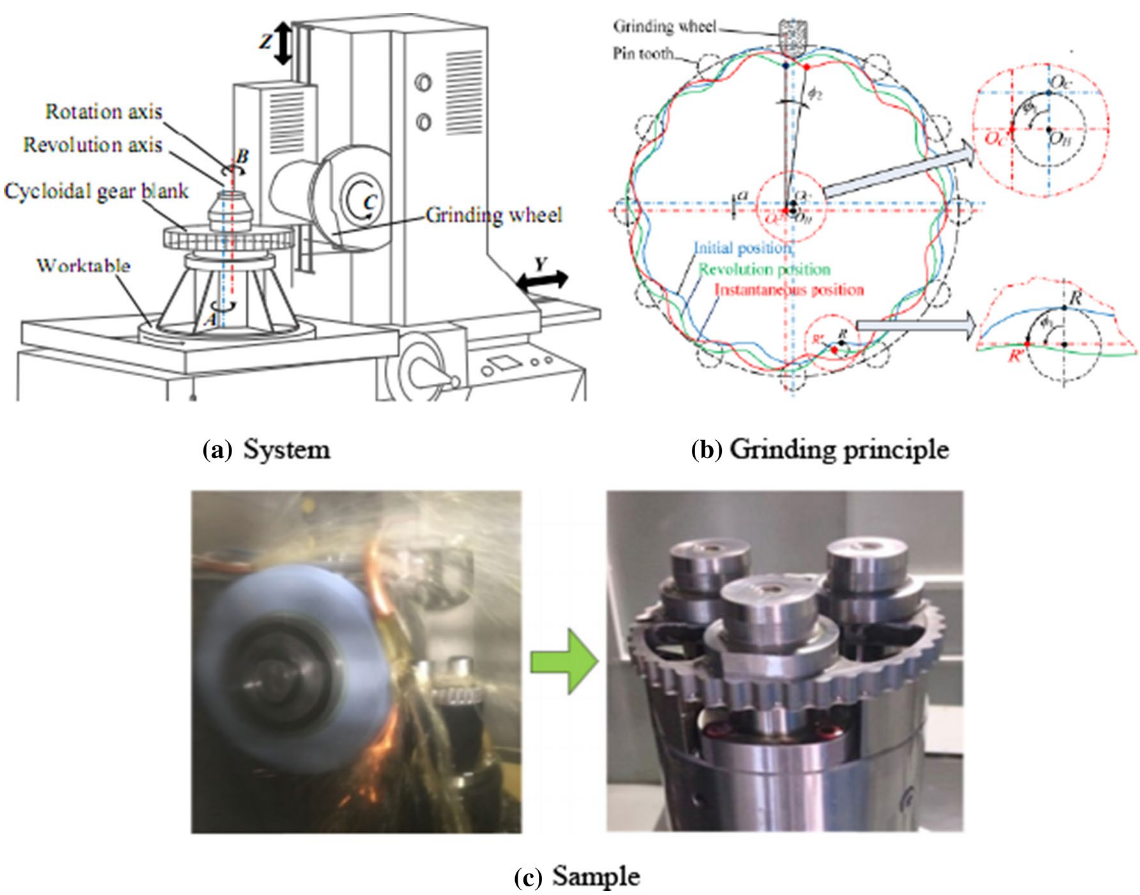

Fig. 11 Grinding system and process for machining the cycloid gear [93]. (open access)

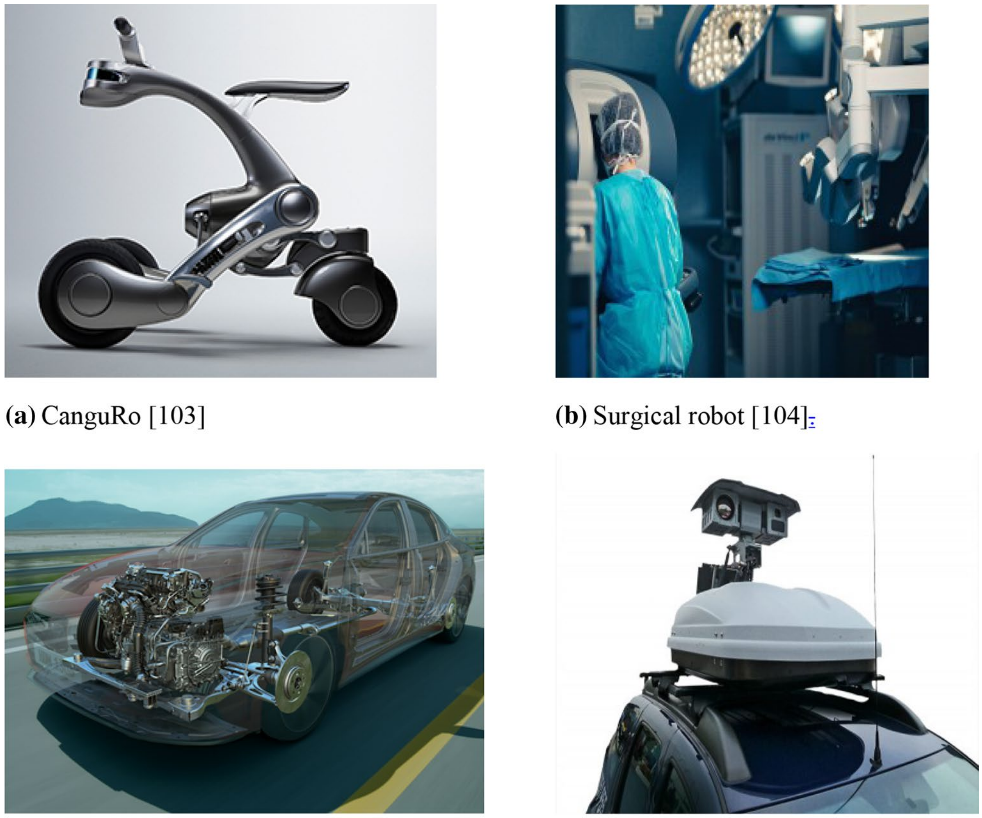

(a) CanguRo [103]

(b) Surgical robot [104].

(c) E-CVVD system in automotive engine [107]

(d) Radar system [108]

Fig. 12 Other applications of the cycloid reducer

7 Conclusion

Although smart manufacturing is a strong industrial driver for reshaping the current competitive landscape and establishing new market leaders, machining manufacturing plays an irreplaceable and dominant role in manufacturing. Machining robots are leading the change in the existing manufacturing system, and the precision reducer is an important component governing the accuracy of the machining robot. The cycloid reducer is the best candidate among precision reducers when considering both the structural compliance and kinematic accuracy of the machining robots. Many types of cycloid reducers have been developed, and numerous design approaches to improve the performance of cycloid reducers have been proposed. Performance evaluations for the cycloid reducer are necessary for validating the proposed designs. In addition, fault detection and diagnosis issues are gaining interest from researchers. Currently, cycloid reducers are finding industrial applications such as in mobility, automotive, and precision industrial robots. Thus, the application of cycloid reducers will continue to expand.

References

1. Davis, J., Edgar, T., Porter, J., Bernaden, J., & Sarli, M. (2012). Smart manufacturing, manufacturing intelligence and demand-dynamic performance. *Computers and Chemical Engineering, 47*, 145–156.
2. Park, K. T., Kang, Y. T., Yang, S. G., et al. (2020). Cyber physical energy system for saving energy of the dyeing process with industrial internet of things and manufacturing big data. *International Journal of Precision Engineering and Manufacturing-Green Technology, 7*, 219–238. https://doi.org/10.1007/s40684-019-00084-7
3. Lee, J., Bagheri, B., & Kao, H.-A. (2015). A Cyber-Physical Systems architecture for Industry 4.0-based manufacturing systems. *Manufacturing letters, 3*, 18–23.
4. Sim, H. S. (2019). Big data analysis methodology for smart manufacturing systems. *International Journal of Precision Engineering and Manufacturing, 20*, 973–982. https://doi.org/10.1007/s12541-019-00136-7
5. Lee, J. Y., Yoon, J. S., & Kim, B. (2017). A big data analytics platform for smart factories in small and medium-sized manufacturing enterprises: An empirical case study of a die casting factory. *International Journal of Precision Engineering and Manufacturing, 18*, 1353–1361. https://doi.org/10.1007/s12541-017-0161-x
6. Tao, F., Qi, Q., Wang, L., & Nee, A. Y. C. (2019). Digital twins and cyber-physical systems toward smart manufacturing and

industry 4.0: Correlation and comparison. *Engineering, 5*(4), 653–661. https://doi.org/10.1016/j.eng.2019.01.014
7. Gupta, N., Tiwari, A., Bukkapatnam, S. T. S., & Karri, R. (2020). Additive manufacturing cyber-physical system: Supply chain cybersecurity and risks. *IEEE Access, 8*, 47322–47333. https://doi.org/10.1109/ACCESS.2020.2978815
8. Mehrpouya, M., Dehghanghadikolaei, A., Fotovvati, B., Vosooghnia, A., Emamian, S. S., & Gisario, A. (2019). The potential of additive manufacturing in the smart factory industrial 4.0: A review. *Applied Science, 9*, 3865.
9. Temoelman, E., Shercliff, H., & Ninaber van Eyben, B. (2014). Additive Manufacturing. In E. Tempelman, H. Shercliff, & B. N. V. Eyben (Eds.), *Manufacturing and design* (pp. 187–200). Butterworth-Heinemann.
10. Jamie, D. (2018). 3D printing vs CNC machining: Which is best for prototyping? https://www.3dnatives.com/en/3d-printing-vs-cnc-160320184/#!
11. Pereira, T., Kennedy, J. V., & Potgieter, J. (2019). A comparison of traditional manufacturing vs additive manufacturing, the best method for the job. *Procedia Manufacturing, 30*, 11–18.
12. Demir, K. A., Doven, G., & Sezen, B. (2019). Industry 5.0 and human-robot co-working. *Procedia Computer Science, 158*, 688–695.
13. Zhu, D., Feng, X., Xu, X., Yang, Z., Li, W., Yan, S., & Ding, H. (2020). Robotic grinding of complex components: A step towards efficient and intelligent machining—Challenges, solutions, and applications. *Robotics and Computer-Integrated Manufacturing, 65*, 101908.
14. Ji, W., & Wang, L. (2019). Industrial robotic machining: A review. *International Journal of Advanced Manufacturing Technology, 103*, 1239–1255.
15. Subrin, K., Sabourin, L., Cousturier, R., Gogu, G., & Mezouar, Y. (2013). New redundant architectures in machining: Serial and parallel robots. *Procedia Engineering, 63*, 158–166.
16. Kim, S. H., Nam, E., Ha, T. I., et al. (2019). Robotic machining: A review of recent progress. *International Journal of Precision Engineering and Manufacturing, 20*(9), 1629–1642.
17. Iglesias, I., Sebastian, M. A., & Ares, J. E. (2015). Overview of the state of robotic machining: Current situation and future potential. *Procedia Engineering, 132*, 911–917.
18. Chen, Y., & Dong, F. (2013). Robot machining: Recent development and future research issues. *International Journal of Advanced Manufacturing Technology, 66*, 1489–1497.
19. Pandremenos, J., Doukas, C., Stavropoulos, P., & Chryssolouris, G. (2011). Machining with robots: A critical review. In *Proceedings of DET2011* (pp. 1–9).
20. Schneider, U., Ansaloni, M., Drust, M., Leali, F., & Verl, A. (2013). Experimental investigation of sources of error in robot machining. In *International workshop on robotics in smart manufacturing (WRSM 2013)* (pp. 14–26).
21. Zhang, T., Yu, Y., Yang, L., Xiao, M., & Chen, S. (2020). Robot grinding system trajectory compensation based on co-kriging method and constant-force control based on adaptive iterative algorithm. *International Journal of Precision Engineering and Manufacturing*. https://doi.org/10.1007/s12541-020-00367-z
22. Schneider, U., Drust, M., Ansaloni, M., Lehmann, C., Pellicciari, M., Leali, F., Gunnink, J. W., & Verl, A. (2014). Improving robotic machining accuracy through experimental error investigation and modular compensation. *International Journal of Advanced Manufacturing Technology, 95*, 83–89.
23. Kuka. (2020). Milling robot. https://www.kuka.com/en-my/products/process-technologies/milling.
24. DePree, J., Gesswein, C. (2008). "Robot machining white paper project", Halcon development, Robotic Industries Association. https://www.robotics.org/robotics/halcyon-development-ria.
25. Klimchik, A., Ambiehl, A., Garnier, S., Furet, B., & Pashkevich, A. (2017). Efficiency evaluation of robots in machining applications using industrial Performance measure. *Robotics and Computer-Integrated Manufacturing, 48*, 12–29.
26. Belaganger-Barrette, M. (2014). Machining with industrial robots. https://blog.robotiq.com/bid/73008/Machining-with-Industrial-Robots.
27. Matsuoka, S., Shimizu, K., Yamazaki, N., & Oki, Y. (1999). High-speed end milling of an articulated robot and its characteristics. *Journal of Materials Processing Technology, 95*, 83–89.
28. Kim, K., Lee, S., Kim, K., et al. (2010). Development of the end-effector measurement system for a 6-axis welding robot. *International Journal of Precision Engineering and Manufacturing, 11*, 519–526.
29. Chen, X., Zhang, Q., & Sun, Y. (2019). Model-based compensation and pareto-optimal trajectory modification method for robotic applications. *International Journal of Precision Engineering and Manufacturing, 20*, 1127–1137.
30. Verl, A., Valente, A., Melkote, S., Brecher, C., Ozturk, E., & Tunc, L. T. (2019). Robots in machining. *CIRP Annuals Manufacturing Technology, 68*, 799–822.
31. Erkaya, S. (2012). Investigation of joint clearance effects on welding robot manipulator. *Robotics and Computer-Integrated Manufacturing, 28*, 449–457.
32. Oh, Y. T. (2011). Influence of joint angular characteristics on the accuracy of industrial robots. *Industrial Robot: An International Journal, 38*(4), 406–418.
33. Giberti, H., Cinquenmani, S., & Legnani, G. (2010). Effect of transmission mechanical characteristics on the choice of a motor-reducer. *Mechatronics, 20*, 604–610.
34. Garcia, P. L., Crispel, S., Saerens, E., Verstraten, T., & Lefeber, D. (2020). Compact gearboxes for modern robotics: A review. *Frontiers in Robotics and AI, 7*(103), 1–19.
35. Harmonic Drive, "Improve the productivity of your factory automation systems with lightweight gears and actuators", 800-921-3332. www.harmonicdrive.net.
36. PhamAhn, A. D. H. J. (2018). High precision reducers for industrial robots driving 4th industrial revolution: State of arts, analysis, design, performance evaluation, and perspective. *International Journal of Precision Engineering and Manufacturing-Green Technology, 5*(4), 519–533.
37. Qin, Z., et al. (2018). A review of recent advances in design optimization of gearbox. *International Journal of Precision Engineering and Manufacturing, 19*(11), 1753–1762.
38. Yang, C., Hu, Q., Liu, Z., et al. (2020). Analysis of the partial axial load of a very thin-walled spur-gear (flexspline) of a harmonic drive. *International Journal of Precision Engineering and Manufacturing, 21*, 1333–1345. https://doi.org/10.1007/s12541-020-00333-9
39. Meng, Y., Wu, C., & Ling, L. (2007). Mathematical modeling of the transmission performance of 2K-H pin cycloid planetary mechanism. *Mechanism and Machine Theory, 42*(7), 776–790.
40. Yu, D. (1987). KHV planetary gearing. *Gear Technology, 4*(6), 21–31.
41. Wang, Y., Qian, Q., Chen, G., Jin, S., & Chen, Y. (2017). Multi-objective optimization design of cycloid pin gear planetary reducer. *Advances in Mechanical Engineering, 9*(9), 1–10. https://doi.org/10.1177/1687814017720053
42. Sun, Z., & Han, L. (2019). A new numerical force analysis method of CBR reducer with tooth modification. *Journal of Physics: Conference Series, 1187*, 032053.
43. Bao, J., & He, W. (2015). Parametric design and efficiency analysis of the output-pin-wheel cycloid transmission. *International Journal of Control and Automation, 8*(8), 349–362.
44. Gear materials. https://khkgears.net/new/gear_knowledge/gear_technical_reference/gear_materials.html.

45. Ovako, Material data sheet -20MnCr5. https://steelnavigator.ovako.com/steel-grades/20mncr5/.
46. Lauer, D. A. (2013). Gear Lubrication. In Q. J. Wang & Y. W. Chung (Eds.), *Encyclopedia of tribology* (pp. 1495–1501). Boston: Springer. https://doi.org/10.1007/978-0-387-92897-5_19
47. Ken bannister. (2017). Understand motor and gearbox lubrication. https://www.efficientplantmag.com/2017/01/understand-motor-gearbox-lubrication/.
48. Botsiber, D. W., & Kingston, L. (1956). Design and performance of the cycloid reducer. *Machine Designs, 28*, 65–69.
49. Blanche, J. G., & Yang, D. C. H. (1989). Cycloid drives with machining tolerances. *ASME Journal of Mechanisms, Transmissions, 111*, 337–344.
50. Litvin, F. L., & Feng, P.-H. (1996). Computerized design and generation of cycloidal gearings. *Mechanism and Machine Theory, 31*(7), 891–911. https://doi.org/10.1016/0094-114x(95)00115-f
51. Hsieh, C.-F. (2014). Dynamics analysis of cycloidal speed reducers with pinwheel and nonpinwheel designs. *Journal of Mechanical Design, 136*(9), 091008. https://doi.org/10.1115/1.4027850
52. Hu, Y., Li, G., Zhu, W., & Cui, J. (2020). An elastic transmission error compensation method for rotary vector speed reducers based on error sensitivity analysis. *Applied Science, 10*, 481.
53. Shin, J. H., & Kwon, S. M. (2006). On the lobe profile design in a cycloid reducer using instant velocity center. *Mechanism and Machine Theory, 41*, 596–616.
54. Tran, T. L., Pham, A. D., & Ahn, H. J. (2016). Lost motion analysis of one stage cycloid reducers considering tolerances. *International Journal of Precision Engineering and Manufacturing, 17*(8), 1009–1016.
55. Chen, B., Zhong, H., Liu, J., Li, C., & Fang, T. (2012). Generation and investigation of a new cycloid drive with double contact. *Mechanism and Machine Theory, 49*, 270–283. https://doi.org/10.1016/j.mechmachtheory.2011.10.001
56. Li, T., Li, J., Deng, X., Tian, M., & Li, Y. (2020). Meshing contact analysis of cycloidal-pin gear in RV reducer considering the influence of manufacturing error. *Journal of the Brazilian Society of Mechanical Sciences and Engineering, 42*, 133. https://doi.org/10.1007/s40430-020-2208-7
57. Hwang, Y.-W., & Hsieh, C.-F. (2007). Determination of surface singularities of a cycloidal gear drive with inner meshing. *Mathematical and Computer Modelling, 45*(3–4), 340–354. https://doi.org/10.1016/j.mcm.2006.05.010
58. Wang, J., Gu, J., & Yan, Y. (2016). Study on the relationship between the stiffness of RV reducer and the profile modification method of cycloid-pin wheel. *Intelligent Robotics and Applications-ICIRA, 2016*, 722–735.
59. Li, T., An, X., Deng, X., Li, J., & Li, Y. (2020). A new tooth profile modification method of cycloidal gears in precision reducers for robots. *Applied Science, 10*, 1266.
60. Ren, Z. Y., Mao, S. M., Guo, W. C., & Guo, Z. (2017). Tooth modification and dynamic performance of the cycloidal drive. *Mechanical Systems and Signal Processing, 85*, 857–866.
61. Bo, W., Jiaxu, W., Guangwu, Z., Rongsong, Y., Hongjun, Z., & Tao, H. (2015). Mixed lubrication analysis of modified cycloidal gear used in the RV reducer. *Proceedings of the Institution of Mechanical Engineers, Part J: Journal of Engineering Tribology, 230*(2), 121–134. https://doi.org/10.1177/1350650115593 30
62. Sun, X., & HanMaLiWang, L. K. L. J. (2018). Lost motion analysis of CBR reducer. *Mechanism and Machine Theory, 120*, 89–106.
63. Lin, W.-S., Shih, Y.-P., & Lee, J.-J. (2014). Design of a two-stage cycloidal gear reducer with tooth modifications. *Mechanism and Machine Theory, 79*, 184–197. https://doi.org/10.1016/j.mechmachtheory.2014.04.009
64. Zang, T., Li, X., Wang, Y., & Sun, L. (2020). A semi-analytical load distribution model for cycloid drives with tooth profile and longitudinal modifications. *Applied Sciences, 10*, 4859.
65. Sensinger, J. W. (2010). Unified approach to cycloid drive profile, stress, and efficiency optimization. *Journal of Mechanical Design, 132*(2), 024503. https://doi.org/10.1115/1.4000832
66. Wang, H., Shi, Z.-Y., Yu, B., & Xu, H. (2019). Transmission performance analysis of RV reducers influenced by profile modification and load. *Applied Science, 9*, 4099.
67. Sun, X., Han, L. J., & Wang. (2019). Design and transmission error analysis of CBR reducer. *Journal of Mechanical Design, 141*, 082301-1–82310.
68. Hsieh, C. F. (2014). The effect on dynamics of using a new transmission design for eccentric speed reducers. *Mechanism and Machine Theory, 80*, 1–16.
69. Pham, A. D., & Ahn, H. J. (2017). Efficiency analysis of a cycloid reducer considering tolerance. *Journal of Friction and Wear, 38*(6), 490–496.
70. Hsieh, C. F. (2015). Traditional versus improved designs for cycloidal speed reducers with a small tooth difference: The effect on dynamics. *Mechanism and Machine Theory, 86*, 15–35.
71. Kumar, N. (2015). Investigation of a driven-train dynamics of mechanical transmissions incorporating cycloidal drives. Ph.D. thesis, Queensland University of Technology, Brisbane.
72. Kosse, V. (2007). Using hysteresis loop and torsional shock load to acess damping and efficiency of cycloid drives. In *Proceedings of 14th international congress on sound & vibration* (*ICSV14*) (pp. 1–8).
73. Yoshioka, T., Hirano, Y., & Ohishi, K. (2014). Vibration suppressing control method of angular transmission error of cycloid gear for industrial robots. In *Proceedings of 2014 international power electronics conference* (pp. 1956–1961).
74. Bednarczyk, S., Jankowski, L., & Krawczyk, J. (2019). The influence of eccentricity changes on power losses in cycloidal gearing. *Tribologia, 3*, 19–29.
75. Xu, L. X., & Yang, Y. H. (2016). Dynamic modeling and contact analysis of cycloid-pin gear mechanism with a turning arm cylindrical roller bearing. *Mechanism and Machine Theory, 104*, 327–349.
76. Xu, L. X., Chen, B. K., & Li, C. Y. (2019). Dynamic modelling and contact analysis of bearing-cycloid-pinwheel transmission mechanisms used in joint rotate vector reducers. *Mechanism and Machine Theory, 137*, 432–458.
77. Dion, J. L., Pawelshi, Z., Chianca, V., Zdzinnicki, Z., Peyret, N., Uszpolewicz, G., Ormezowski, J., & Mitukiewicz, G. (2020). Theoretical and experimental study for an improved cycloid drive model. *Journal of Applied Mechanics, 87*, 011002-1–11013.
78. Bao, J., He, W., Qiao, S., & Johnson, P. (2020). Optimum design of parameters and contact analysis of cycloid drive. *Journal of Computational Methods in Sciences and Engineering, 21*, 71–83.
79. Tsai, Y. T., & Lin, K. H. (2020). Dynamic analysis and reliability evaluation for an eccentric speed reducer based on fem. *Journal of Mechanics, 36*(3), 395–403. https://doi.org/10.1017/jmech.2019.52
80. Yu, H. L., Yi, J. H., Hu, X., & Shi, P. (2013). Study on teeth profile modification of cycloid reducer based on non-Hertz elastic contact analysis. *Mechanics Research Communications, 48*, 87–92.
81. Yang, Y., Chen, C., & Wang, S. (2018). Response sensitivity to design parameters of RV reducer. *Chinese Journal of Mechanical Engineering, 31*, 49. https://doi.org/10.1186/s10033-018-0249-y
82. Neagoe, M., Diaconescu, D., Pascalse, L., & Saulescu, R. (2007). On the efficiency of a cycloidal planetary reducer with a modified structure. *International Conference on Economic Engineering and Manufacturing Systems ICEEMS, 8*(3), 544–549.

83. Ahn, H. J., Choi, B. M., Lee, Y. H., & Pham, A. D. (2021). Impact analysis of tolerance and contact friction on a RV reducer using FE method. *International Journal of Precision Engineering and Manufacturing*. https://doi.org/10.1007/s12541-021-00537-7
84. Zang, Y., He, W., Wang, X., & Luo, Y. (2019). Transmission error simulation analysis for RV reducer with orthogonal experiment method. *Intelligent Robotics and Applications-ICIRA, 2019*, 629–641.
85. Kim, K. H., Lee, C. S., & Ahn, H. J. (2009). Torsional rigidity of a cycloid drive considering finite bearing and Hertz contact stiffness. *International Power Transmission and Gearing Conference, 6*, 125–130.
86. Olejarczyk, K., Wikło, M., & Kołodziejczyk, K. (2019). The cycloidal gearbox efficiency for different types of bearings—Sleeves vs. needle bearings. *Proceedings of the Institution of Mechanical Engineers, Part C: Journal of Mechanical Engineering Science, 233*(21–22), 7401–7411. https://doi.org/10.1177/0954406219859903
87. Liu, Z., Zhang, T., Wang, Y., et al. (2019). Experimental studies on torsional stiffness of cycloid gear based on machining parameters of tooth surfaces. *International Journal of Precision Engineering and Manufacturing, 20*(6), 1017–1025. https://doi.org/10.1007/s12541-019-00108-x
88. Pham, A. D., Tran, T. L., & Ahn, H. J. (2017). Hysteresis curve analysis of a cycloid reducer using non-linear spring with a dead zone. *International Journal of Precision Engineering and Manufacturing, 18*(3), 375–380.
89. Gorla, C., Davoli, P., Rosa, F., Longoni, C., Chiozzi, F., & Samarani, A. (2008). Theoretical and experimental analysis of a cycloidal speed reducer. *Journal of Mechanical Design, 130*(11), 112604-112604–8.
90. Mihailidis, A., Athanasopoulos, E., & Agouridas, K. (2016). EHL film thickness and load dependent power loss of cycloid reducers. *Proceedings of the Institution of Mechanical Engineers, Part C, 230*(7–8), 1303–1317.
91. Baron, P., Kočiško, M., Dobránsky, J., Pollák, M., & Cmorej, T. (2015). Research and correlation of diagnostic methods for assessment of the state of oil filling in cycloid gearbox. *Advances in Materials Science and Engineering, 2015*, 1–9. https://doi.org/10.1155/2015/597841
92. Wang, S., Tan, J., Gu, J., & Huang, D. (2020). Study on torsional vibration of RV reducer based on time-varying stiffness. *Journal of Vibration Engineering and Technologies*. https://doi.org/10.1007/s42417-020-00211-8
93. Chen, C., & Yang, T. (2017). Structural characteristics of rotate vector reducer free vibration. *Shock and Vibration, 4214370*, 1–14. https://doi.org/10.1155/2017/4214370
94. Li, T., Li, J., Deng, X., Tian, M., & Li, Y. (2020). Quantitative correction method for the grinding errors of cycloidal gears in precision reducer. *Journal of Advanced Mechanical Design, Systems, and Manufacturing, 14*(4), 1–14.
95. Gu, L., Xu, J., & Luo, S. (2016). The design of new cycloid gear with variable cross section and the research of end milling in five-axis machine tool. *Manufacturing Technology, 16*(3), 497–502.
96. Maeng, S., Lee, P. A., Kim, B. H., et al. (2020). An analytical model for grinding force prediction in ultra-precision machining of WC with PCD micro grinding tool. *International Journal of Precision Engineering and Manufacturing-Green Technology*. https://doi.org/10.1007/s40684-020-00199-2
97. Chu, X., Xu, H., Wu, X., Tao, J., & Shao, G. (2018). The method of selective assembly for the RV reducer based on genetic algorithm. *Proceedings of the Institution of Mechanical Engineers, Part C: Journal of Mechanical Engineering Science, 232*(6), 921–929. https://doi.org/10.1177/0954406217700179
98. Bai, B., Li, Z., & Zhang, J. (2019). Failure rate prediction and reliability assessment of RV reducer. In *International conference on quality, reliability, risk, maintenance, and safety engineering* (*QR2MSE*) (pp. 364–371).
99. Kim, Y., et al. (2020). Phase-based time domain averaging (PTDA) for fault detection of a gearbox in an industrial robot using vibration signals. *Mechanical Systems and Signal Processing, 138*(106544), 1–19.
100. Zhang, Y., et al. (2019). Industrial robot rotate vector reducer fault detection based on hidden Markov models. In *IEEE international conference on robotics and biomimetics (ROBIO)* (pp. 3013–3018).
101. An, H., Liang, W., Zhang, Y., Li, Y., Liang, Y., & Tan, J. (2017). Rotate vector reducer crankshaft fault diagnosis using acoustic emission techniques. In *5th International conference on enterprise systems* (ES). https://doi.org/10.1109/es.2017.55.
102. Lee, K., Hong, S., & Oh, J. (2020). Development of a lightweight and high-efficiency compact cycloidal reducer for legged robots. *International Journal of Precision Engineering and Manufacturing, 21*(3), 415–425. https://doi.org/10.1007/s12541-019-00215-9
103. Yamato, H., Ogihara, K., et al. (2020). A partner robot transforming to a vehicle: CanguRo-design, development and evaluation of its in-wheel drive unit with cycloid gear. In *Proceedings of 2020 IEEE/SICE international symposium on system integration* (pp. 1205–1211).
104. FuRo (2007). CanguRo: intelligent robot–transformable and ridable. https://furo.org/en/works/canguro/canguro.html.
105. Spinea, Spinea–Excellence in motion: Applications-medial. https://www.spinea.com/en/industries/medical.
106. Lee, S., & Baek, S. W. (2020). A study on the improvement of the cam phase control performance of an electric continuous variable valve timing system using a cycloid reducer and BLDC motor. *Microsystem Technology, 26*, 59–70. https://doi.org/10.1007/s00542-019-04411-5
107. Kia Motor. (2015). Kia Stinger: Engine control system/E-CVVT motor. http://www.kstinger.com/e_cvvt_motor-464.html.
108. Austin, M. (2019). How Hyundai's new, more fuel-efficient CVVD engine technology works. https://www.caranddriver.com/news/a28284180/hyundai-cvvd-car-engine-technology-explained/.
109. Spinea, Spinea–Excellence in motion: Applications-defence and security. https://www.spinea.com/en/industries/defense-and-security.

Anh-Duc Pham received a Ph.D. degree from Soongsil University, Korea in 2018. He was a research associate in the IMSLab – Soongsil University and is currently a researcher/lecturer at the Faculty of Mechanical Eng., University of Science and Technology- The University of Danang. Dr. Pham's research interests are in the area of mechatronics, control & precision machine design, sustainable design & manufacturing, applications of Nanomaterials.

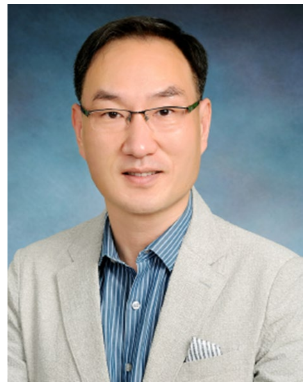

Hyeong-Joon Ahn received B.S., M.S. and Ph.D. degrees from Seoul national university, Korea in 1995, 1997 and 2001, respectively. He was research associate in University of Virginia, 2002 and is currently a professor at School of Mechanical Eng., Soongsil University. Dr. Ahn's research interests are in the area of mechatronics, sensors, actuators, control and precision machine design.